Intelligent Robots and Autonomous Agents
Ronald C. Arkin, editor

Behavior-Based Robotics, Ronald C. Arkin, 1998

Robot Shaping: An Experiment in Behavior Engineering, Marco Dorigo and Marco Colombetti, 1998

Layered Learning in Multiagent Systems: A Winning Approach to Robotic Soccer, Peter Stone, 2000

Evolutionary Robotics: The Biology, Intelligence, and Technology of Self-Organizing Machines, Stefano Nolfi and Dario Floreano, 2000

Reasoning about Rational Agents, Michael Wooldridge, 2000

Introduction to AI Robotics, Robin R. Murphy, 2000

Strategic Negotiation in Multiagent Environments, Sarit Kraus, 2001

Mechanics of Robotic Manipulation, Matthew T. Mason, 2001

Mechanics of Robotic Manipulation

Matthew T. Mason

A Bradford Book
The MIT Press
Cambridge, Massachusetts
London, England

This book was set in Times-Roman by the author and was printed and bound in the United States of America.

Library of Congress Cataloging-in-Publication Data

Mason, Matthew T.
Mechanics of robotic manipulation / Matthew T. Mason.
p. cm.—(Intelligent robotics and autonomous agents)
"A Bradford book."
Includes bibliographical references and index.
ISBN 0-262-13396-2 (hc. : alk. paper)
1. Manipulators (Mechanism). 2. Robotics. I. Title. II. Series.

TJ211 .M345 2001
629.8'92—dc21 2001030226

Contents

Figure 6.10
The three positive regions have no common intersection, nor do the three negative regions. Hence the labeled regions are null, the possible resultants are all of wrench space, and the triangle is in force closure.

deformable bodies. For the problem as stated, we have force closure, we *may* have static equilibrium, but we surely would not classify it as stable.

EXAMPLE 3: A TRIANGLE IN FORCE CLOSURE

Consider a three-finger grasp of a triangle in the plane (figure 6.10). Kinematic analysis, or force analysis using frictionless contact, suggest that the triangle is not securely grasped, that is, that there are some loads that cannot be balanced by the contact forces. However, with sufficient frictional forces, the possible resultants exhaust all of wrench space, and the triangle is in force closure. The figure shows the moment labeling of the problem. The reader may easily verify that both the positive-labeled and the negative-labeled regions are empty. Thus there are no constraints on the possible wrenches: force closure.

6.6 Planar sliding

Some manipulation tasks involve an object sliding on a planar support surface. The mechanics of planar sliding apply to problems as diverse as moving furniture (section 7.2) and fixturing objects for machining operations. This section develops expressions for the frictional force and moment of planar sliding, and introduces an elegant graphical representation known as the *Limit Surface*.

The motion of a pushed object is often indeterminate. If a rigid object is supported by more than three contact points, the distribution of support forces is underdetermined. If the frictional forces are assumed proportional to the normal forces, as Coulomb suggests, then the frictional forces are also underdetermined. The problem is illustrated by the defective dinner plate of figure 6.11. The plate was designed with a circular ridge on the bottom, so that the support forces would be concentrated at the edge of the plate. Unfortunately, the bottom of the plate sagged during the firing process, so that the center is also in contact

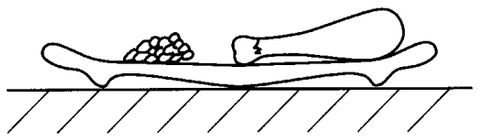

Figure 6.11
It is impossible to predict the motion of this plate, without knowing the distribution of support forces between the plate and the table.

with the planar support. There is no way to predict whether the support forces will be concentrated at the center, giving it an irritating tendency to rotate, or at the edge, resisting rotation. In practice, the plate's behavior will depend on details that may be very difficult to model. It may behave well with a tablecloth, and poorly without a tablecloth. Its behavior might depend on the phase of the moon. (Tidal forces induce microscopic changes in the shapes of the plate and table.)

The defective dinner plate is a particularly egregious example of the indeterminacy of planar sliding. In the worst case the problem can be very awkward, but in most practical situations there are many ways of addressing the problem. One inescapable conclusion is that a useful theory of planar sliding should capture this indeterminacy, which is a primary goal for the approach described below.

The first step is to develop expressions for the force and moment of planar sliding under the assumption that the support forces are known and described by a finite *pressure distribution* $p(\mathbf{r})$. Under those assumptions indeterminacy is not an issue—there is a one-to-one mapping between the direction of slider motion and the resulting wrench, except when the slider is motionless.

Given the force and moment for a known finite pressure distribution, the next step is to generalize to cases where there may be finite force concentrated at an isolated point of support, corresponding to infinite pressure. In those cases the mapping between direction of slider motion and the resulting wrench may be many-to-one or one-to-many.

Finally, we also have to consider the indeterminacy arising from an unknown or partially known pressure distribution, such as the dinner plate example above, which is addressed in chapter 7.

Force and moment of planar sliding

Let some object be in planar motion, supported by a fixed planar surface. Choose a coordinate frame with the x-y plane coincident with the support, and z pointing outward. Let the object's contact with the surface be confined to some region R. Let $\mathbf{r}$ be the position vector of some point in the object, and let $\mathbf{v}(\mathbf{r})$ be the velocity of that point. If $p(\mathbf{r})$ is the

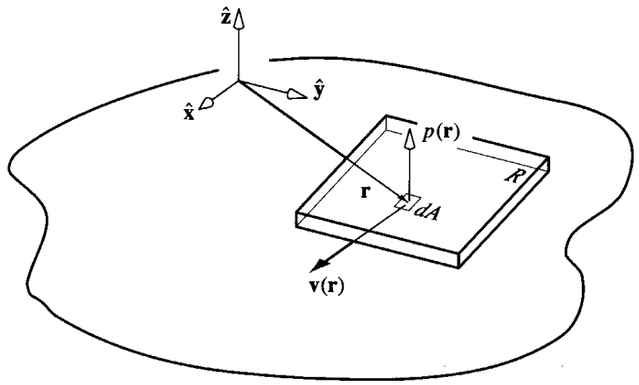

Figure 6.12
Notation for planar sliding.

pressure at $\mathbf{r}$, and dA a differential element of area at $\mathbf{r}$, then the magnitude of the normal force at $\mathbf{r}$ is given by

$$p(\mathbf{r})\,dA \tag{6.11}$$

and Coulomb's law gives us the tangential force at $\mathbf{r}$:

$$-\mu \frac{\mathbf{v}(\mathbf{r})}{|\mathbf{v}(\mathbf{r})|} p(\mathbf{r})\,dA \tag{6.12}$$

for $|\mathbf{v}(\mathbf{r})| \neq 0$, where μ is the coefficient of friction, assumed uniform over the contact region R.

Integrating over R, we obtain expressions for the total force and moment due to friction:

$$\mathbf{f}_f = -\mu \int_R \frac{\mathbf{v}(\mathbf{r})}{|\mathbf{v}(\mathbf{r})|} p(\mathbf{r})\,dA \tag{6.13}$$

$$\mathbf{n}_f = -\mu \int_R \mathbf{r} \times \frac{\mathbf{v}(\mathbf{r})}{|\mathbf{v}(\mathbf{r})|} p(\mathbf{r})\,dA \tag{6.14}$$

Note that the frictional force $\mathbf{f}_f$ lies in the x-y plane, and the total frictional moment $\mathbf{n}_f$ acts along the z-axis. Without knowledge of the pressure distribution $p(\mathbf{r})$, these integrals cannot be evaluated, leading to indeterminacy in the frictional forces. There is an exception, though: pure translation.

CASE 1: PURE TRANSLATION

If the object is in pure translation, all points are moving in the same direction, and we can factor the integrals of equations 6.13 and 6.14.

$$\mathbf{f}_f = -\mu \frac{\mathbf{v}(\mathbf{r})}{|\mathbf{v}(\mathbf{r})|} \int_R p(\mathbf{r})\,dA \tag{6.15}$$

$$\mathbf{n}_f = -\mu \int_R \mathbf{r}\, p(\mathbf{r})\,dA \times \frac{\mathbf{v}(\mathbf{r})}{|\mathbf{v}(\mathbf{r})|} \tag{6.16}$$

Let $\mathbf{f}_0$ be the total normal force, and let $\mathbf{r}_0$ be the centroid of the pressure distribution. Then

$$f_0 = \int_R p(\mathbf{r})\,dA \tag{6.17}$$

$$\mathbf{r}_0 = \frac{1}{f_0} \int_R \mathbf{r}\, p(\mathbf{r})\,dA \tag{6.18}$$

Substituting into equations 6.15 and 6.16,

$$\mathbf{f}_f = -\mu \frac{\mathbf{v}(\mathbf{r})}{|\mathbf{v}(\mathbf{r})|} f_0 \tag{6.19}$$

$$\mathbf{n}_f = \mathbf{r}_0 \times \mathbf{f}_f \tag{6.20}$$

Hence the frictional forces distributed over the support region have a resultant, with magnitude μf_0, in a direction opposing the motion, through the centroid $\mathbf{r}_0$. In other words, the force is equivalent to that obtained by applying Coulomb's law to the sliding of a single point located at $\mathbf{r}_0$.

DEFINITION 6.1: The **center of friction** is the centroid $\mathbf{r}_0$ of the pressure distribution.

THEOREM 6.1: For a rigid body in purely translational sliding on a planar surface, with uniform coefficient of friction, the frictional forces reduce to a force through the center of friction, opposing the velocity.

Proof Given above. ■

In some cases, the center of friction is easily determined. If an object is at rest on the support plane, with no applied forces other than gravity and the support contact forces, then the center of friction is directly below the center of gravity. This is the only location that allows the contact forces to balance the gravitational force. We can generalize slightly, allowing additional applied forces, as long as they are in the support plane. We can also

permit accelerated motion of the body, if the center of gravity is in the support plane. But acceleration of a body whose center of gravity is above the support plane will, in general, cause a shift in the pressure distribution, and a corresponding shift in the center of friction. Applied forces not lying in the support plane will generally cause a similar shift.

CASE 2: ROTATION

Now suppose that the body is rotating, with an instantaneous center $\mathbf{r}_{IC}$. Then the velocity of a point at $\mathbf{r}$ is given by

$$\mathbf{v}(\mathbf{r}) = \omega \times (\mathbf{r} - \mathbf{r}_{IC}) \tag{6.21}$$

$$= \dot{\theta}\,\hat{\mathbf{k}} \times (\mathbf{r} - \mathbf{r}_{IC}) \tag{6.22}$$

and the direction of motion at $\mathbf{r}$ is

$$\frac{\mathbf{v}(\mathbf{r})}{|\mathbf{v}(\mathbf{r})|} = \operatorname{sgn}(\dot{\theta})\,\hat{\mathbf{k}} \times \frac{\mathbf{r} - \mathbf{r}_{IC}}{|\mathbf{r} - \mathbf{r}_{IC}|} \tag{6.23}$$

Substituting into equations 6.13 and 6.14 we obtain

$$\mathbf{f}_f = -\mu \operatorname{sgn}(\dot{\theta})\,\hat{\mathbf{k}} \times \int_R \frac{\mathbf{r} - \mathbf{r}_{IC}}{|\mathbf{r} - \mathbf{r}_{IC}|} p(\mathbf{r})\,dA \tag{6.24}$$

$$n_{fz} = -\mu \operatorname{sgn}(\dot{\theta}) \int_R \mathbf{r} \cdot \frac{\mathbf{r} - \mathbf{r}_{IC}}{|\mathbf{r} - \mathbf{r}_{IC}|} p(\mathbf{r})\,dA \tag{6.25}$$

Notice that these equations have a well-defined limit as the rotation center $\mathbf{r}_{IC}$ approaches infinity, so they apply to pure translations as well as rotations.

The Limit Surface

The form of equations 6.24 and 6.25 suggests a functional relationship between the slider's rotation center and the resulting frictional force. However, if we allow non-zero support force at a discrete point, then these equations are undefined for rotations about the support point. For this reason the relation between slider motion and frictional force cannot generally be described as a function. Fortunately there is an elegant description of the motion–force mapping: the *limit surface* introduced by Goyal, Ruina, and Papadopoulos (1991).

To develop the limit surface, we first consider sliding of a single particle. Let $\mathbf{v}$ be the velocity of the particle, and let $\mathbf{f}$ be the frictional force applied *by the particle to the support surface*. Note that this convention is the opposite of our usual convention, and corresponds to a sign change on the force $\mathbf{f}$. We will use the term *frictional load* when referring to the frictional force applied by the slider to the support surface.

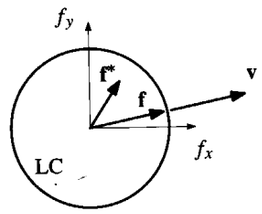

Figure 6.13
Limit curve for a point slider. Adapted from (Goyal et al., 1991).

For our point slider, we can express Coulomb's law as follows:

slip: $\mathbf{f} \parallel \mathbf{v}$, and $|\mathbf{f}| = \mu f_n$, where μ is the coefficient of friction, and f_n is the support force.

stick: $|\mathbf{f}| \leq \mu f_n$.

We can develop an equivalent graphical representation of Coulomb's law. Consider the set of all frictional loads that can be applied by the point slider. This set is a disc comprising all forces acting through the point with magnitude no greater than μf_n. This set is bounded by a circle of radius μf_n at the origin of force space, which we define to be the *limit curve* LC (see figure 6.13). Now we can say that the frictional load $\mathbf{f}$ must satisfy the *maximum power inequality*:

$$\forall_{\mathbf{f}^* \in LC}\ (\mathbf{f} - \mathbf{f}^*) \cdot \mathbf{v} \geq 0 \tag{6.26}$$

In other words, the motion $\mathbf{v}$ yields a load that is extremal in the $\mathbf{v}$ direction.

More significantly, we note that when slip occurs the load $\mathbf{f}$ is on the limit curve, and the motion $\mathbf{v}$ is *normal* to the limit curve at $\mathbf{f}$.

Now we consider sliders with extended support. Let $\mathbf{r}$ vary over the support region, and construct a limit curve $LC(\mathbf{r})$ at each point $\mathbf{r}$, so that at each point the maximum power inequality holds:

$$\forall_{\mathbf{f}^*(\mathbf{r}) \in LC(\mathbf{r})}\ (\mathbf{f}(\mathbf{r}) - \mathbf{f}^*(\mathbf{r})) \cdot \mathbf{v}(\mathbf{r}) \geq 0 \tag{6.27}$$

Now let $\mathbf{p}$ be the total frictional load wrench

$$\mathbf{p} = \begin{pmatrix} f_x \\ f_y \\ n_{0z} \end{pmatrix} = \sum_{\mathbf{r}} \begin{pmatrix} f_x(\mathbf{r}) \\ f_y(\mathbf{r}) \\ \mathbf{r} \times \mathbf{f}(\mathbf{r}) \end{pmatrix} \tag{6.28}$$

and let $\mathbf{q}$ be the velocity twist

$$\mathbf{q} = \begin{pmatrix} v_{0x} \\ v_{0y} \\ \omega_z \end{pmatrix} \tag{6.29}$$

Now, for some given motion $\mathbf{q}$, let $\mathbf{f}(\mathbf{r})$ be a distribution of frictional loads satisfying Coulomb's law, and let $\mathbf{f}^*(\mathbf{r})$ be some arbitrary distribution, satisfying only the constraint that at each $\mathbf{r}$, $\mathbf{f}^*(\mathbf{r})$ is in the corresponding limit curve:

$$\forall_r \quad \mathbf{f}^*(\mathbf{r}) \in \mathrm{LC}(\mathbf{r}) \tag{6.30}$$

Let $\mathbf{p}$ and $\mathbf{p}^*$ be the total frictional load wrench for $\mathbf{f}(\mathbf{r})$ and $\mathbf{f}^*(\mathbf{r})$ respectively. Now, we can describe the power dissipated by $\mathbf{f}(\mathbf{r})$ in either of two ways, yielding the equation

$$\mathbf{p} \cdot \mathbf{q} = \sum_{\mathbf{r}} \mathbf{f}(\mathbf{r}) \cdot \mathbf{v}(\mathbf{r}) \tag{6.31}$$

Similarly we can write

$$\mathbf{p}^* \cdot \mathbf{q} = \sum_{\mathbf{r}} \mathbf{f}^*(\mathbf{r}) \cdot \mathbf{v}(\mathbf{r}) \tag{6.32}$$

Taking the difference yields

$$(\mathbf{p} - \mathbf{p}^*) \cdot \mathbf{q} = \sum_{\mathbf{r}} (\mathbf{f}(\mathbf{r}) - \mathbf{f}^*(\mathbf{r})) \cdot \mathbf{v}(\mathbf{r}) \tag{6.33}$$

Since the maximum power inequality must be satisfied at every point $\mathbf{r}$, every term in the sum on the right hand side is non-negative. Thus we obtain a maximum power inequality for the total frictional load wrench:

$$(\mathbf{p} - \mathbf{p}^*) \cdot \mathbf{q} \geq 0 \tag{6.34}$$

To summarize, to find the true frictional load, we can start with the set of all load distributions satisfying the constraint that at each point $\mathbf{r}$ the magnitude of the load must be no greater than $\mu f_n(\mathbf{r})$, and then choose a distribution that yields maximum power.

When the slider is not moving, any load distribution $\mathbf{f}^*(\mathbf{r})$ is possible, subject only to the constraint that at each point the magnitude of the load must be no greater than $\mu f_n(\mathbf{r})$. Form the set of all possible total frictional load wrenches $\mathbf{p}^*$, and define the *limit surface* to be the surface of this set. Then we can summarize the maximum power inequality by stating that the frictional load wrench during slip yields maximum power over all wrenches in the limit surface. It follows that during slip the total frictional load wrench $\mathbf{p}$ lies on the limit surface, and the velocity twist $\mathbf{q}$ is normal to the limit surface at $\mathbf{p}$.

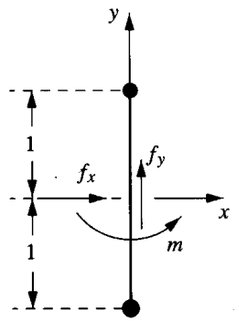

Figure 6.14
Sliding barbell. Adapted from (Goyal et al., 1991).

We state several properties of the limit surface without proof. The limit surface is closed, convex, and encloses the origin of wrench space. It is symmetric when reflected through the origin. Its orthogonal projection onto the f_x, f_y plane is a circle of radius $\sum \mu f_n$.

If the pressure distribution is everywhere finite, i.e. with no discrete points of support, then the limit surface is strictly convex, and the velocity twist to frictional load wrench mapping is one-to-one.

The more interesting cases involve discrete support points. If there are such points, then there are flat facets on the limit surface. At such a facet, several different loads give rise to the same motion—rotation about the discrete support point.

An even more interesting case arises when the support region R degenerates to a line or a subset of a line. In this case the limit surface is no longer smooth. At a vertex of the limit surface several different motions can produce the same frictional load. This corresponds to those motions with rotation centers collinear with all points of support.

The limit surface has uses that go well beyond what can be described here. It applies to some non-isotropic friction laws, such as ice skates or ratchet wheels. It yields insights into the dynamic motion of sliders, and, as we shall see it provides insights into the mechanics of quasistatic manipulation.

Example

Figure 6.14 shows a planar slider with just two points of support, a *barbell*. We assume the barbell's weight is evenly divided between the two support points. Figure 6.15 shows the corresponding limit surface. It was constructed by the following steps:

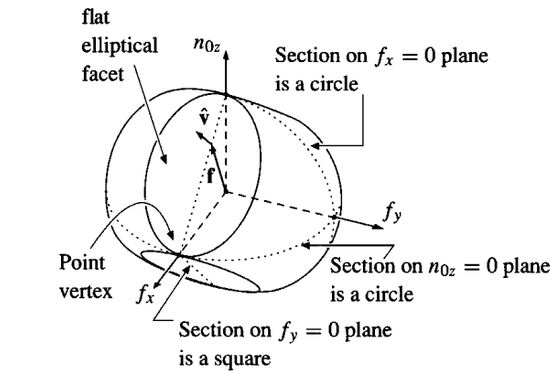

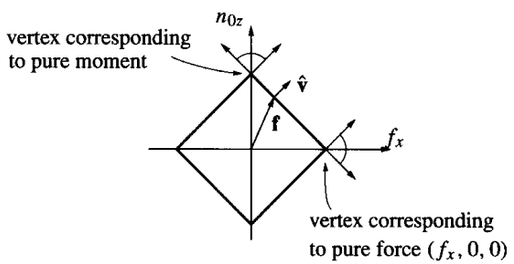

Figure 6.15
Barbell limit surface. Adapted from (Goyal et al., 1991).

1. Construct the limit surface LS_a comprising all force loads arising at support point a. If a were at the origin this would be a disc in the $n_{0z} = 0$ plane. But since a is not at the origin, LS_a is an elliptical disc in the $n_{0z} - f_x = 0$ plane.
2. Similarly, construct the limit surface LS_b. It also is an elliptical disc, this time in the $n_{0z} + f_x = 0$ plane.
3. The desired limit surface is the Minkowski sum of LS_a and LS_b. In other words it is the set $\{\mathbf{w}_a + \mathbf{w}_b \mid \mathbf{w}_a \in \mathrm{LS}_a, \mathbf{w}_b \in \mathrm{LS}_b\}$.

The barbell's limit surface illustrates many of the properties of limit surfaces. There are four flat facets, where the frictional load may vary while the normal remains stationary.

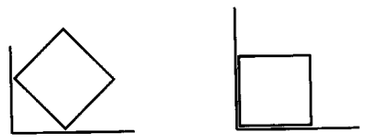

Figure 6.16
Two block in corner problems for exercise 6.2.

This implies many different loads mapping to a single motion, which occurs when the barbell rotates about one of the support points. There are four such facets, one for each of two possible rotation directions about each of two different support points.

There are also four vertices, where the frictional load is stationary as the normal may vary. This implies many different motions mapping to a single frictional load, which occurs for a rotation about a point collinear with the two support points.

Elsewhere the limit surface is smooth and strictly convex, so the load–motion mapping is one-to-one.

6.7 Bibliographic notes

Many engineering mechanics texts provide good introductions to Coulomb friction. Gillmor (1971) and Truesdell (1968) provide some interesting historical notes on Coulomb, Amontons, and da Vinci. Simunovic (1975) was the first to analyze peg insertion using friction cones. Erdmann (1984) was the first to construct composite friction cones in wrench space. Prescott (1923) and MacMillan (1936) developed expressions for force and moment of planar sliding, and introduced the center of friction. The particular treatment of planar sliding is taken from (Mason, 1986). The limit surface is taken from (Goyal, 1989; Goyal, Ruina, and Papadopoulos, 1991). See (Howe and Cutkosky, 1996) for experimental evaluation, application, and approximations related to the limit surface.

Exercises

Exercise 6.1: Analyze the pipe clamp using the moment labeling method, and the force dual method: find the possible resultants of the contact forces, and characterize the set of load forces that would be balanced.

Exercise 6.2: Use the moment labeling and the force dual methods to analyze each of the problems in figure 6.16. A block is in the corner of a fixed tray, and you are to identify the